UNIVERSITY OF TARTU
Faculty of Science and Technology
Institute of Molecular and Cell Biology

Oleksandra Dranova

The role of TGFBI in wound healing and skin regeneration

Bachelor's Thesis (12 ECTS)

Curriculum Science and Technology

Supervisor(s):
PhD Mariliis Klaas
PhD Kristina Mäemets-Allas

Tartu 2021

The role of TGFBI in wound healing and skin regeneration

Abstract: The skin is an essential organ of any mammalian organism. It performs many different functions, such as sensory, metabolic, thermoregulatory function, and others. One of the most important functions of the skin is to create a barrier between the body and the environment. Processes such as skin regeneration and wound healing are fundamental to the normal functioning of the body. This research investigates the effect of Transforming Growth Factor Beta Induced Protein (TGFBI) on skin regeneration and wound healing through its ability to modulate cell migration and proliferation. Fibroblasts and immortalized human keratinocytes were used during the experiments. The immunofluorescence analysis of mouse skin tissue samples showed that TGFBI is expressed both in healthy and healing skin, namely in the dermis. Experiments with cultured skin cells showed that TGFBI does not affect the migration and proliferation of keratinocytes and fibroblasts.

Keywords: skin, wound healing, skin regeneration, extracellular matrix, TGFBI, cell migration, cell proliferation, fibroblasts, keratinocytes.

CERCS: B210 (Histology, cytochemistry, histochemistry, tissue culture)

Pealkiri eesti keeles (title in Estonian)

Lühikokkuvõte: Nahk on imetajate oluline elund. Nahal on mitmeid olulisi funktsioone nagu tunnetus, ainevahetu- ja termoregulatsioon ning mitmeid teisi. Üks olulisematest naha funktsioonidest on luua barjäär keha ja keskkonna vahele. Protsessid nagu naha regeneratsioon ja haava paranemine on aluseks keha normaalsele funktsioneerimisele. Käesolev töö uurib transformeeriva kasvufaktori beeta poolt inditseeritud valgu (TGFBI) efekti naha regeneratsioonile ning haava paranemisele läbi rakkude migratsiooni ja proliferatsiooni mõjutamise. Eksperimentides kasutati fibroblaste ja inimese immortaliseeritud keratinotsüüte. Koeproovide immunofluorestentsanalüüsi tulemusena selgus, et TGFBI ekspresseerub nii terves hiire nahas kui ka paranevas haavas peamiselt dermises. Katsete tulemusel leiti, et TGFBI ei mõjuta keratinotsüütide ja fibroblastide migratsiooni ja proliferatsiooni.

Võtmesõnad: nahk, haavade paranemine, naha taastumine, rakuväline maatriks, TGFBI, rakkude migratsioon, rakkude proliferatsioon, fibroblastid, keratinotsüüdid.

CERCS: B210 (Histoloogia, tsütokeemia, histokeemia, koekultuurid.

TABLE OF CONTENTS:

TERMS, ABBREVIATIONS AND NOTATIONS

BSA - Bovine Serum Albumin

DMEM - Dulbecco's Modified Eagle Medium

DTT - dithiothreitol

ECM - extracellular matrix

FBS - Fetal Bovine Serum

FGF - fibroblast growth factor

GAGs - anionic glycosaminoglycans

HF PCR - High fidelity polymerase chain reaction

HFSC - hair follicle stem cells

ITS - Insulin-Transferrin-Selenium

LB media - Luria-Bertani

NBT/BCIP solution - nitro-blue tetrazolium chloride/5-bromo-4-chloro-3’-indolyl phosphate p-toluidine salt solution

NF H2O - nuclease free water

PBS - Phosphate Buffered Saline

PDGF - platelet-derived growth factor

PEG40000 - polyethylene glycol M=40000g/mol

PFS - paraformaldehyde solution

PVDF membrane - polyvinylidene fluoride membrane

Pen-Strep - Penicillin-Streptomycin solution

SDS - Sodium dodecyl sulfate

TAE buffer - Tris-acetate-EDTA

TBS - Tris-Buffered Saline

TEMED - Tetramethylethylenediamine

TGF-β - Transforming Growth Factor Beta

TGFBI - Transforming Growth Factor Beta Induced Protein

UV radiation - ultraviolet radiation

Vasodilation - widening of blood vessels

Angiogenesis - formation of new blood vessels

Myogenic spasm - contraction of blood vessel

INTRODUCTION

Skin is an essential organ of any mammalian organism. Through interaction with the environment, the skin performs a number of essential functions such as thermoregulatory, sensory, metabolic, protective, excretory, and others (Timmons, 2006). The skin is usually divided into three main layers: epidermis, dermis and hypodermis. The epidermis and dermis, in turn, can also be divided into several other layers. Each layer of the skin contains cells of a certain type. The predominant cells of the epidermis are keratinocytes, which create a mechanical barrier of the skin through their constant proliferation. In the dermis, fibroblasts are the most abundant cells, secreting procollagen and elastic fibers that give the skin structure and elasticity (Lawton, 2019; Smith, 2019).

The skin is a fairly strong structure, however it can be damaged. In response to injury and to ensure cutaneous homeostasis, regeneration and wound healing processes are activated in skin. There are many factors influencing these processes. During this Bachelor's thesis research the effect of the Transforming Growth Factor Beta Induced Protein (TGFBI) on the migration and proliferation of fibroblasts, which are actively involved in the process of skin regeneration and wound healing was examined. TGFBI is released in the extracellular matrix of a large number of tissues and can influence the wound healing process through the ability to bind extracellular matrix molecules to each other. It is also believed that TGFBI is involved in the processes of morphogenesis, adhesion / migration, angiogenesis, and inflammation. (Nummela *et al*., 2012; Reinboth *et al.*, 2006).

This Bachelor's project is part of a larger research theme of Dr. Viljar Jaks research group (Institute of Molecular and Cell Biology, University of Tartu) that aims to characterize potentially regeneration-promoting ECM proteins in skin. It was hypothesized that TGFBI influences the process of skin regeneration and healing by accelerating cell migration and proliferation.

1. LITERATURE REVIEW

1.1 Mammalian skin overview

All mammals are covered by skin, the largest organ of the body, which accounts for approximately 15% of the total body weight (Kanitakis, 2001). Mammalian skin is the layer of typically soft, adaptable external tissue that interfaces with the environment. Skin is a significant organ because it performs numerous valuable functions, such as protection, sensation, thermoregulation, as well as metabolic and excretory function (Timmons, 2006).

By protecting the organism from physical trauma, harmful effects of UV radiation, bacteria and toxins skin functions as a mechanical barrier, as well as a diffusion barrier that lessens water loss that could lead to dehydration of an organism. Protecting the body from freezing or overheating, as well as maintaining a constant body temperature, occurs due to a change in blood flow through the cutaneous vascular bed. When the ambient temperature is high, we tend to sweat due to vasodilation, which leads to increased blood flow and heat loss in the body. On the contrary, at low temperatures, blood vessels narrow, blood flow is weakened, preventing the body from losing heat. (Lawton, 2019)

When thinking about the metabolic function of the skin, it is worth mentioning the ability of the skin to synthesize vitamin D in the presence of UV light. Urea, water and other waste products can be excreted by skin. In addition to that, sebaceous glands, which are located in the dermis, produce a mixture of lipids, called sebum. It protects skin by serving as an antibacterial agent. (Monteiro-Riviere, 2005)

1.1.1 Histological structure of skin

The skin of mammals is separated into many distinct layers. These layers are the epidermis, dermis, and hypodermis, also known as subcutaneous tissue, which is a connective tissue mostly composed of fat cells rather than the skin layer (Figure 1) (Lawton, 2019).

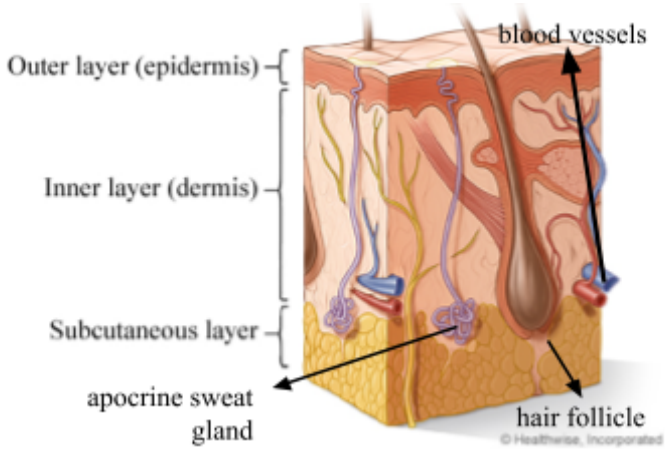

Figure 1. Cross section of the skin, skin layers. This figure is adapted from https://myhealth.alberta.ca/Health/pages/conditions.aspx?hwid=tp10137

1.1.1.1 Epidermis

Epidermis is the upper layer of skin that covers and protects the body. Its primary purpose is to build a mechanical shield between the organism and the environment. Thickness of the epidermis depends on the body parts. Epidermis is thinner in areas where the hairline is dense, and thicker in areas where the hairline is sparse (Monteiro-Riviere, 2005). According to Lawton (2019), epidermis is primarily composed of keratinocytes, which account for more than 80% of all cells in the epidermal layer. Epidermis also consists of such cells as melanocytes, Langerhans cells and Merkel cells, which are known as non keratinocytes (Monteiro-Riviere, 2005; Zeng *et al*., 2017).

There are four main layers of the epidermis (from bottom to top): *stratum basale* (the basal cell layer), *stratum spinosum* (squamous cell layer), *stratum granulosum* (the granular cell layer), and *stratum corneum* (the cornified or horny cell layer) (Kolarsick *et al*., 2011; Zeng *et al*., 2017). According to Monteiro-Riviere (2005) and Lawton (2019) there is another layer of the epidermis, found between the granular and cornified layers, is known as the transparent layer or *stratum lucidum*, it exists only in areas of the body where the skin is the thickest.

The *stratum basale* is the lowest layer of the epidermis and adheres to the dermis. Basal layer is made up of stem cells called basal cells, which will differentiate into keratinocytes (Watt, 1998). This basal cell layer contains stem cells that express proliferative antigens, such as Ki67 and PCNA, while keratinocytes express keratins (K5, K14/K15) (Losquadro, 2017; Kanitakis, 2001; Moll *et al*., 1982). The cells of *stratum basale* are arranged in a single cell row along the basement membrane. They are cuboid in form and have large

oval nuclei. Basal cells are attached to each other and to the upper layer of the epidermis (*stratum spinosum*) by desmosomes and by hemidesmosomes to the basement membrane (Barbiery *et al*., 2014). Basal layer keratinocytes are effectively capable of mitotic division, which allows them to give rise to new daughter cells, which in turn regenerate the epidermis. Under normal conditions, it requires around a month for basal layer cells to migrate to the upper layers of the epidermis. Skin damage, for example, can influence the rate of keratinocyte proliferation (Kolarsick *et al*., 2011). Among the basal keratinocytes, melanocyte cells are equally distributed in the basal layer (1 melanocyte for 4-10 keratinocytes).

Melanocytes produce the main skin pigment called melanin. They migrate into the epidermis, originating from the neural crest. Melanocytes can be recognised with antibodies identifying melanocyte-specific antigens. Merkel cells are also present in the basal cell layer but with low density. Merkel cells are linked to keratinocytes via their plasma membrane desmosomes. These cells can be distinguished due to expression of specific antigens, including keratin n°20, chromogranin, synaptophysin and various neuropeptides. (Kanitakis, 2001)

The *stratum spinosum* is the skin layer above the basal layer. This layer is made up of 5-10 cell layers, and depending on where the keratinocytes are located, they could have different shapes and perform different functions (Barbiery *et al*., 2014). Cells adjacent to the basal layer, for example, have round nuclei and a versatile shape, while cells in the upper layers of *stratum spinosum* have a flattened shape. Desmosomes link the cells in the squamous layer, which helps to keep the epidermis intact (Kolarsick *et al*., 2011). Langerhans cells, which are specialized macrophages, are found among the keratinocytes in this layer. Their primary role is to absorb foreign particles and damaged cells. Langerhans cells contain a specific cytoplasmic marker, the Birbeck granule, originating from the cell membrane, while keratinocytes express K1 and K10 keratins. As new keratinocytes are formed in the basal layer, the cells of this layer move to the next, overlying granular cell layer (Biga *et al*., 2019; Kanitakis, 2001).

The cells in the granular layer are arranged in three to five layers and become flatter. This layer's keratinocytes secrete large amounts of keratins (K2e and K11, etc.) and keratohyalin protein, which is accumulated in the cells as lamellar granules. These proteins are responsible for the granular appearance of that kind of layer. (Biga *et al*., 2019; Kanitakis, 2001) In order to develop a waterproof barrier, the granular layer's keratinocytes release Odland bodies and keratinosomes in addition to lamellar granules.

As cells mature and move to the upper layers of the epidermis, they begin to prepare for the degradation of their organelles and nucleus; this process is aided by the presence of lysosomal enzymes in the granular layer. (Barbieri *et al*., 2014)

As it was previously stated, the *stratum lucidum* is only found on areas of the body where the skin is particularly thick, such as the palms and feet (Timmons, 2010). The transparent layer is a thin layer of dead keratinocytes bound by the protein eleidene, which gives this layer a translucent appearance. It is located between the *stratum granulosum* and the s*tratum corneum.* This layer's primary role is to reinforce the epidermis and also provide additional protection. (Biga *et al*., 2019)

The *stratum corneum*, or topmost layer of the epidermis, is made up of completely differentiated dead and flattened cells called corneocytes. Corneocytes in this layer bind with a complex mixture of lipids and proteins cleaved by keratinocyte enzymes, leading to the formation of the skin's lipid barrier (Lawton, 2019). This layer is known as the skin's primary mechanical barrier, preventing excessive water loss as well as excessive percutaneous absorption (Chu, 2012; Lawton, 2019).

1.1.1.2 Dermis

The dermis is a layer of mesenchymal connective tissue situated deep inside the epidermis and overlying the subcutaneous fat layer (Lopez-Ojeda *et al*., 2020). This skin layer tends to be 15-40 times thicker than epidermis (Barbieri *et al*., 2014). The dermis is mostly fibrous and composed of collagen and elastic fibers. Hyaluronic acid, proteoglycans, and glycoproteins - are all components of an amorphous extracellular “base material” which is located between the fibrous components. Dermis provides structural and nutritional support, as well as a constant body temperature thanks to the work of vasoactive dermal vessels. (Brown and Krishnamurthy, 2020) The majority of the dermal constituents are of mesodermal origin, with the exception of nerves, which, including melanocytes, are derived from the neural crest (Smith and Holbrook, 1986). The dermis is divided into two layers: the thin, brittle papillary dermis and the thicker, deeper reticular dermis. The papillary dermis is located underneath the dermoepidermal junction and is made up of freely arranged collagen fibers. The reticular dermis is made up of thick collagen bundles that extend parallel to the surface of the skin. (Kanitakis, 2001)

The most popular cells in the dermis are fibroblasts. They produce procollagen and elastic fibers. Procollagen is essential because it is subsequently converted to collagen by enzymes that catalyze it. Fibroblasts are present in both layers of the dermis, but they are

more common in the papillary dermis. The function of collagen is to create a fibrous network consisting of fibroblasts which helps new cells grow. Collagen is also essential for replacing dead skin cells (Smith, 2019). There are several ways to distinguish fibroblasts within other cells. For instance, one can detect them using antibodies that detect pan-mesenchymal markers, such as vimentin or Te7 antigen. Another way to determine fibroblasts is with enzymes that take part in collagen synthesis, such as proline-4-hydroxylase (Kanitakis, 2002).

Other cell types in dermis are: mast cells and vascular smooth muscle cells. Mast cells store chemicals which are needed in case a cell is damaged. Vascular smooth muscle cells play a role in body temperature homeostasis by contracting and dilating blood vessels (Smith, 2019).

1.1.1.3 Hypodermis

Hypodermis, also known as the subcutaneous fat layer, is the lowest layer of skin under the dermis. The hypodermis is responsible for thermoregulation, mechanical defense, and the ability to store nutrients. The hypodermis is mostly made up of adipose tissue and loose connective tissue, and its main function is to connect the dermis to a nearby muscle or bone (Kanitakis, 2001; Monteiro-Riviere, 2005). Adipocytes are the primary hypodermis cells with lipid cytoplasm. Fibrous septa, which include veins, arteries, and nerves, isolate adipocyte cells (Barbieri *et al*., 2014; Kanitakis, 2001). Leptin hormone is secreted by adipocytes and tends to provide a long-term feedback signal that controls fat mass (Haake *et al*., 2001). Macrophages and fibroblasts are two other types of hypodermis cells (Wong *et al*., 2015).

1.1.2 Skin homeostasis

Keratinization is the mechanism by which keratinocytes differentiate and migrate through all layers of the epidermis, from the basal layer to the stratum corneum. Keratinocytes, in turn, differentiate from interfollicular epidermal stem cells (keratinocyte stem cells) (Monteiro-Riviere, 2005). The persistent proliferation of keratinocytes in the basal layer causes them to migrate "up" and thus renew the epidermis on a regular basis. Corneocytes are keratinocytes that have undergone total differentiation; this process means complete cell death, but it is fundamentally distinct from the process of programmed cell death, apoptosis (Houben *et al*., 2006). During this process, keratinocytes enlarge due to an

increase in the volume of cytoplasm and differentiation products (tonofilaments, keratohyalin granules and lamellar granules) in them. As the contents of the cells increase, their nuclei and organelles disintegrate, eventually forming the stratum corneum of protein-rich cells containing fibrous keratin and keratohyalin (Eckert *et al*., 2002; Monteiro-Riviere, 2005).

Due to the presence of hair on the body, a protective shield against external stimuli is created, and a steady body temperature is maintained. Hair follicles are one of the few organs in the body that regenerate in a cyclic pattern. The hair follicle is made up of an epithelial cylinder (made up of keratinocytes and dermal papilla mesenchymal cells) and a dermal sheath. In a cyclic manner hair follicles go through development (anagen), involution (catagen), and rest phases (telogen). The regeneration of hair follicles is dependent on epithelial-mesenchymal interactions and is driven by alternate activation of hair follicle stem cells (HFSC). (Chen *et al*., 2020; Ji *et al*., 2021)

1.2 Wound healing

Wound healing is an important and complex physiological process to restore the integrity of the skin. During the formation of a wound, a number of cellular and molecular mechanisms are initiated in the body, as a result of which, under normal conditions, complete wound healing and restoration of the skin occurs. All the mechanisms that are activated during the healing process are closely intertwined with each other, however, several main stages of wound healing can be distinguished. These stages are hemostasis, inflammation, proliferation and tissue remodelling (Figure 2). (Young and McNaught, 2011; Kirsner *et al*., 1993)

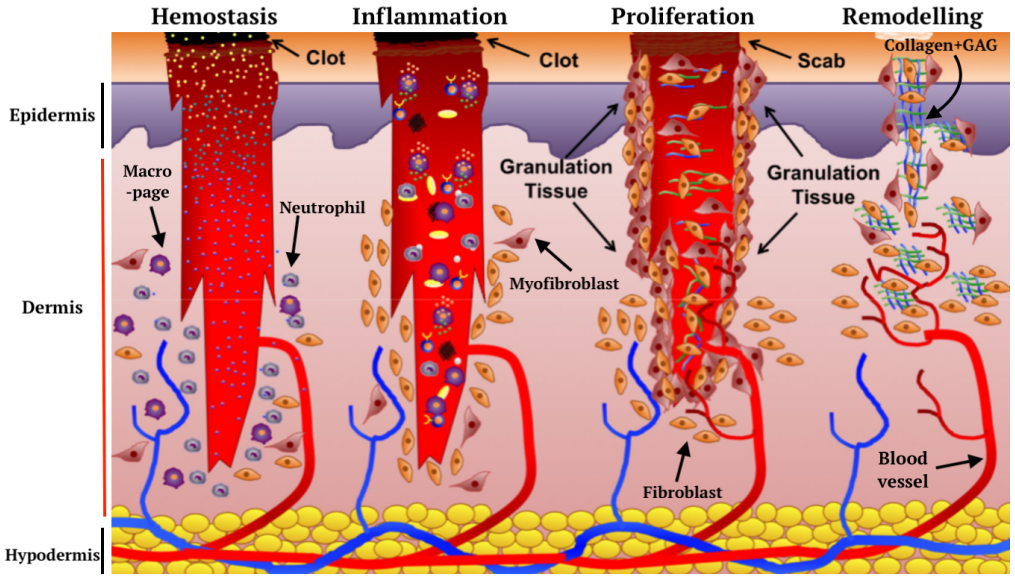

Figure 2. Phases of wound healing process. Figure adapted from Melott *et al*., 2016.

Hemostasis (immediately after injury)

Any type of injury causes blood vessel damage. Hemostasis is a physiological process that occurs in a wound shortly after it is formed. This mechanism's primary goal is to prevent exsanguination (Timmons, 2010). Damaged blood vessels are immediately constricted by smooth muscle contraction after an injury. Smooth muscle contractions are triggered by receiving signals from adjacent cells, a nerve reflex, and myogenic spasm. A blood plug forms after the bleeding has stopped. The blood clot is formed when platelets come into contact with exposed fibrillar collagen; this plug also contains thrombin and fibronectin; all of these factors release cytokines and other growth factors, which activate the inflammatory process and contribute to the wound healing process. (Broughton *et al*., 2006).

Inflammation (up to 6 days after injury)

The formation of inflammation is critical in the wound healing process. The primary function of this mechanism is to rid the wound bed of all foreign bodies in order to prevent infection (Strodtbeck, 2001). The inflammatory phase is divided into two stages: early and late. The complement cascade is activated during the early inflammatory phase, and the molecular mechanisms of this cascade facilitate the arrival of neutrophils at the site of injury. TGF-β proteins, complement components (C3a and C5a), and formylmethionyl peptides are all produced by platelet products and bacteria, and they all attract neutrophils to the wound site. Neutrophils have phagocytic activity, which means they can destroy

bacteria and dead cells inside the wound. When the risk of infection is no longer present, neutrophils undergo apoptosis and are replaced by macrophages. (Velnar *et al*., 2009)
Macrophages are monocytes that have been differentiated and play a significant role in the late inflammatory phase. They continue to perform a phagocytic function and in addition release cytokines (platelet-derived growth factor (PDGF), TGF-β, fibroblast growth factor (FGF), etc.), which are important for inducing cell proliferation and migration, as well as matrix formation (Gonzalez *et al*., 2016; Young and McNaught, 2011).

Proliferation (day 4-14)

As it was previously stated, all phases of the wound healing process are strongly intertwined and, to some extent, proceed in parallel. The proliferative process comes after the possibility of infection in the wound has been eliminated. This process involves the formation of new blood vessels (angiogenesis), the synthesis of new epithelium at the wound site (re-epithelialization), and the formation of granular tissue to fill the wound bed (Strodtbeck, 2001). Platelets release growth factors such as TGF-b, PDGF, and FGF during the formation of a platelet plug. These growth factors, combined with hypoxia, cause the onset of angiogenesis. In turn, a hypoxic gradient forms between the wound's edges, to which the vessels are adjacent, and its non-vascular center.
As the wound vascularizes, it becomes filled with new thin blood vessels formed from the branches of healthy ones. Endothelial cells, which form blood vessels, are the primary cells in this process (Young and McNaught, 2011).
Re-epithelialization is the next mechanism of the proliferative phase. Keratinocytes undergo active mitotic division and migrate from the wound's edges to form a new epithelial layer under the influence of locally secreted growth factors and cytokines. Contact inhibition stops keratinocyte division and migration as soon as they form a uniform cell layer (Strodtbeck, 2001). Growth factors TGF-b and PDGF stimulate fibroblast proliferation and migration into the wound, where they accumulate. Fibroblasts then deposit extracellular matrix proteins (proteoglycans, fibronectins, and hyaluronan) in the wound and subsequently produce collagen and fibronectin. Granular tissue is made up of these deposits as well as newly formed vessels that replace the previously formed blood clot (Timmons, 2010; Young and McNaught, 2011).

Remodelling (up to 1 year or more)

The remodeling process is the final stage of wound healing, and its main goal is to form a healthy epithelium and a scar in order to ensure the full possible tensile strength of the healed skin region. The newly formed granular tissue remodels and matures into a scar during this process. The number of cells and blood vessels in scar tissue decreases as it forms, while the number of collagen fibers increases. (Gonzalez *et al*., 2011)

Also, the organisation of collagen is changing; initially developed type III collagen will be replaced by type I collagen, creating a balance between newly synthesized and degraded collagen. Newly healed tissue is frail and can never exceed the strength level of healthy skin. A newly epithelialized wound is weak and will never exceed the strength level of healthy skin. However, as a result of the collagen reorganization process, the tensile strength improves over time and according to Strodtbeck (2001) can approach 80 percent of the strength of normal tissue (Schultz *et al*., 2011).

1.3 Overview of the extracellular matrix

The extracellular matrix (ECM) connects all cells in the body and keeps them in close contact with it (Hynes, 2009). For maintenance of tissue homeostasis, differentiation and morphogenesis, the ECM is able to activate various significant biochemical and biomechanical signals. By binding various growth factors and interacting with cell-surface receptors to evoke signal transduction and control gene transcription, the ECM manages important morphological organization and physiological function. ECM properties tend to vary from tissue to tissue (Frantz *et al*., 2010). ECM is a three-dimensional complex and dynamic structure made up of a large number of matrix molecules that differ from tissue to tissue. The ECM is thought to be divided into two major forms that vary structurally as well as in terms of constituent components, these types are interstitial and pericellular. Intercellular matrices surround cells, while pericellular matrices adjoint and are in near proximity to them (Theocharis *et al*., 2016). Collagens, proteoglycans, elastin, and glycoproteins are the primary components of the ECM (Yue, 2014; Theocharis *et al*., 2016; Labat-Robert *et al*., 1990).

The most common proteins in the ECM are collagen proteins. Fibroblasts, myofibroblasts, osteoblasts, and chondrocytes primarily synthesize and secrete them in the ECM (Bosman and Stamenkovic, 2003). There are 28 known forms of collagens in vertebrates, which are

classified as fibril-forming collagens (types I, II, III), mesh-forming collagens (type IV), collagens associated with fibrils with interruptions in their triple helices (IX, XII), and others (Yue, 2014). In most tissues, collagen type I and II are thought to be the key components of the ECM. They bind to other collagens, ECM proteins, and proteoglycans, forming fibrillar structures that then bind to interconnected ECM molecules, resulting in a complex three-dimensional matrix network. Collagens tend to provide structural, shaping and organisational support (Bosman and Stamenkovic, 2003; Theocharis *et al*., 2016).

Proteoglycans are glycosylated proteins with covalently bound high anionic glycosaminoglycans (GAGs), the forms of which are found in many connective tissue extracellular matrices (Yanagishita, 1993). Proteoglycans are classified into several families, each of which serves a particular purpose. Aggrecan, versican, neurocan, and brevican are examples of lecticans. They provide tissue elasticity and thus serve a structural role (Bosman and Stamenkovic, 2003; Yanagishita, 1993). Decorin, biglycan, fibromodulin, and keratocan are proteoglycans that guide the formation of collagen networks. Decorin may also affect the activity of the transforming growth factor beta. The heparan sulphate proteoglycan family is also important; it is divided into matrix (perlecan and agrin) and membrane-associated proteoglycans (syndecan and glypican). Membrane-associated heparan sulphate proteoglycans affect cell adhesion, proliferation, migration, and differentiation during wound healing. (Bosman and Stamenkovic, 2003; Yue, 2014)

Another essential component of the ECM is elastin. Elastin is a stable and insoluble polymer that is responsible for the elasticity of fabrics. In mammals, elastin is secreted as a monomer of tropoelastin and is encoded by a single gene (Wise and Weiss, 2009; Yue, 2014). The ability of elastin to stretch is restricted by its close connection with collagen fibrils (Frantz *et al*., 2010).

Glycoproteins are equally important components of the extracellular matrix due to their ability of linking all of the matrix's components into a single network through interactions with each other, collagens, proteoglycans, and some specific cell membrane molecules. Fibronectin, laminin, tenascin, undulin, thrombospondins, and entactin are the most essential extracellular matrix glycoproteins (Schuppan and Riecken, 1990; Yue, 2014).

1.4 Overview of TGFBI

Transforming Growth Factor Beta Induced Protein (TGFBI) is also referred to as βig-H3 or keratoepithelin. This protein is secreted by the extracellular matrix of several tissues, with the exception of the brain and induced by transforming growth factors (TGF-1 and TGF-2) (Zhao *et al*., 2002). TGFBI has a molecular weight of 68 kDa and is made up of 683 amino acids. An N-terminal secretory signal peptide, a cysteine-rich domain (EMI), four fasciclin-1 repeating domains (FAS1-1...FAS1-4), Arg-Gly-Asp integrin binding motif (RGD) at the C-terminus, and NKDIL and EPDIM motifs (Ween *et al*, 2012). Schematic structure of TGFBI is shown on Figure 3.

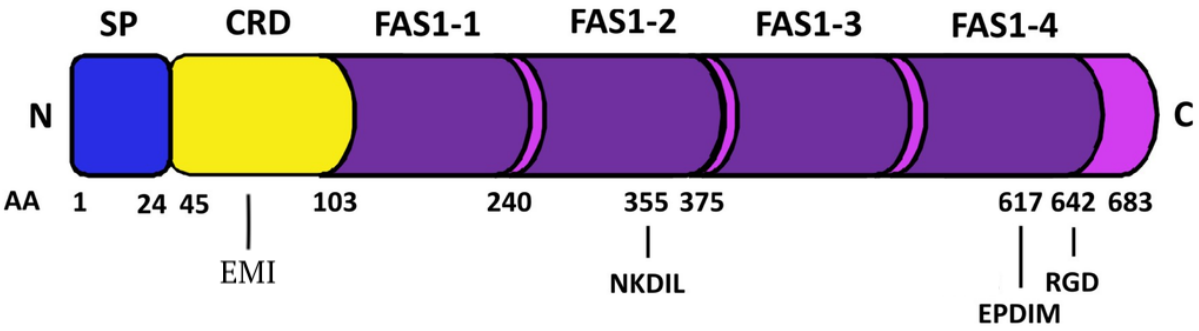

Figure 3. Schematic structure of Transforming Growth Factor Beta Induced Protein. Figure is adapted from Ween *et al*., 2012.

TGFBI has been found in the ECM of developing and mature endothelial cells in human vascular tissues, papillary dermis, primary spongiosa, periosteum, and perichondrium (O'Brien *et al*., 1996; LeBaron *et al*., 1995). TGFBI is involved in a number of physiological processes, including morphogenesis, adhesion/migration, angiogenesis, and inflammation. It also has an effect on wound healing (Nummela *et al*., 2012). TGFBI has the ability to bind extracellular matrix molecules with one another, thus acting as a linker protein. Furthermore, by binding to collagen types I, II, and IV, it facilitates cell-collagen interaction (Reinboth *et al*., 2006).

In keratinocytes, fibroblasts, chondrocytes, osteoblasts and endothelial cells TGFBI protein is involved in migration and adhesion. When it comes to adhesion, the effect is controlled by interaction with various integrins through integrin-binding motifs in the βig-H3 protein (Thapa *et al*., 2005).

TGFBI protein has been linked to a variety of diseases like diabetic nephropathy, atherosclerosis, various cancers, and rheumatoid arthritis. However, this protein has

received the most attention in the context of various corneal disorders (Ween *et al*., 2012). The mutated TGFBI encourages turbid material accumulation in the superficial cornea, which leads to the degradation of epithelial adhesion, resulting in painful erosions and visual impairment (Runager *et al*, 2008).

When it comes to the impact of protein TGFBI on tumorigenesis, there are two major theories. Many studies show that TGFBI acts as a tumor suppressor and inhibits tumorigenesis. However, these findings are contradicted by others, which claim that TGFBI promotes tumorigenesis. TGFBI, for example, is abundantly expressed in lung cancer, pancreatic cancer cell lines and tissues, squamous cell carcinoma of the oral cavity, human colon carcinoma, and other cancers. (Ween *et al*., 2012)

According to other studies, TGFBI inhibits tumorigenesis and is thought to act as a tumor suppressor. TGFBI expression is also decreased in a variety of tumor cells (neoplastically transformed fibroblasts, radiation-induced epithelial cells of the bronchi, etc.). TGFBI expression in tumors is likely to be explained by mechanisms such as hypermethylation of the TGFBI promoter region and interstitial deletion (loss of chromosome 5q) (Thapa *et al*., 2007; Ween *et al*., 2012).

2. THE AIMS OF THE THESIS

In order to confirm or refute the hypothesis of the current research, stating that **TGFBI has an effect on skin regeneration and wound healing** the following aims were put forward in this thesis:

- Characterize the expression of TGFBI in the wound healing process
- Examine TGFBI effect on cell migration
- Examine TGFBI effect on cell proliferation

3. EXPERIMENTAL PART

3.1 Materials and methods

All manuals were provided by supervisors Mariliis Klaas and Kristina Mäemets-Allas.

3.1.1 Cloning

High fidelity polymerase chain reaction (HF PCR) (Applied Biosystems, No. 2720) was performed according to manufacturer's guidelines in order to ensure a high degree of replication accuracy of the DNA of interest (TGFBI). PCR reaction mixture consisted of 5x HF buffer, 10mM dNTP mix, TGFBI cloning primers (Cl_HindIII_TGFBI_forw 5′ cccAAGCTTATGGCGCTCTTCGTGCGGCTGCTG 3′, Cl_XhoI_TGFBI_rev 5′ cggCTCGAGCTAATGCTTCATCCTCTCTAATAAC 3′ (10 nM), commercial TGFBI plasmid (Sino Biological, Germany) with concentration of 119,3 ng/µl, fusion polymerase and nuclease free H2O. The PCR programme was running for 35 cycles in a such manner: 30 seconds at 98°C for the first denaturation, 10 seconds at 98°C for the denaturation, 30 seconds at 60°C for the annealing, 1 minute at 72°C for the DNA synthesis and 10 more minutes at 72°C for the additional DNA synthesis. Agarose gel (Lonza, USA), consisting of 1x TAE buffer (50 ml), agarose (1%) and of ethidium bromide (1µg/ml) for gel electrophoresis was prepared during the DNA amplification process. Amplified PCR product was loaded into the gel, as well as 4 µl 1kb GeneRuler (Thermo Scientific, Lithuania) to enable the determination of DNA sequence length. The gel was running for approximately 25 minutes at 100 V. When the gel was ready, it was placed under the UV light to confirm the presence of the correct sequence of interest (~2000 bp). Later the PCR product of interest was cut from the gel and purified with MicroElute GEL/PCR Purification Kit (Favorgen, USA) according to manufacturer's protocol. Piece of the gel was immediately dissolved in 500 µl of FADF buffer and incubated at 55°C up to full dissolution of the gel piece (5-10 minutes). The resulting mixture was transferred to a filter tube (tube with a FADF filter) and centrifuged at 15000 rpm for 1 minute to get rid of the flow-through. 750 µl of Washing buffer (contains ethanol) was added into the FADF filter and again centrifuged for one minute at the same speed. After centrifugation, the flow-through was discarded and the tube was centrifuged one more time at 15000 rpm for 3 minutes for drying. When that step was done, FADF filter was transferred to a new Eppendorf tube and 40 µl of Elution buffer was added onto the filter membrane to elute the TGFBI PCR

product from the filter via centrifugation at 15000 rpm for 1 minute.

To create DNA ends suitable for ligation the TGFBI PCR product and pcDNA3.1 plasmid were restricted with the enzymes HindIII and XhoI overnight at 37°C. After that restriction products were separated on the 1% agarose gel, the plasmid and PCR products were cut out and purified from the gel (as described above). Purified TGFBI and pcDNA plasmid were ligated as follows: ligation mix and vector control were done. Ligation mix consisted of TGFBI and pcDNA plasmids, ligation buffer (500 mM Tris-HCl, 100 mM $MgCl_2$, 50 mM dithiothreitol DTT, 10 mM ATP, pH 7.6) and a T4 ligase. Vector control consisted of the same components, however, instead of TGFBI plasmid, NF H2O was added to it. After mixing all the components by pipetting, ligation mixes were incubated for 1 hour at room-temperature. After the incubation recombinant plasmid and vector control mixes were ready to be inserted into DNA-competent bacteria.

3.1.2 Bacterial transformation and plasmid purification

Bacterial transformation was done using DH5α competent bacterial cells. Initially cell suspension was kept on ice for 25 minutes and later transferred into Eppendorf tubes in equal amounts (50µl). The TGFBI ligation mix (10 µl) was added to the first tube and pcDNA vector control (0,5 µl) to the second. Both mixtures were incubated on ice for 15 minutes and given the hot shock at 42°C for 2 minutes and transferred on ice one more time for cooling down for 2 minutes more. Then 500 µl of Luria-Bertani (LB) media was added to both tubes and cells were left to grow for 1 hour at 37°C to activate the ampicillin gene in bacteria. After 1 hour tubes were spined at 6000 rpm for 1 minute. Almost all supernatant was discarded from the tubes, only 50-100 µl was left and the pellets were resuspended in it. Resulting cell suspensions were transferred onto 10 cm Petri dishes with LB media and ampicillin on them. Cells were left to overnight growth at 37°C.

During the next day, the regular PCR was done in order to check the presence of sequence of interest (TGFBI). 10 colonies containing TGFBI and 2 colonies containing pcDNA vector control were picked and each separately mixed with 2µl of Green Buffer (Thermo Fisher Scientific, Lithuania), MQ water (7 µl) and Reverse/Forward primers (0,5 µl). The PCR programme was the same as described above. Samples were loaded into the gel, 1 more well was loaded with 50 bp ladder and another well was loaded with water mix to ensure the negative control. The gel was running at 100 V. After it was done, results were

visualised under the UV light and the colonies with correct sequence length (~220 bp) were picked from the Petri dish and placed into 100 ml tubes containing LB media for additional overnight growth at 37°C.

On the next day, before starting the purification kit, cell suspensions were transferred to 50 ml plastic tubes and centrifuged at 5100 rpm for 5 minutes at 16°C. The flow-through was later discarded, and the cell pellets were left to dry for a couple of minutes. At that moment it was possible to start the process of plasmid purification. The plasmid purification was done by using NucleoBond Xtra Maxi Endotoxin-free (EF) kit (Macherey-Nagel).

Cell pellets were completely resuspended in 8 ml of Resuspension Buffer RES-EF+RNase by pipetting. After that cells were lysed in 8 ml of Lysis Buffer LYS EF and mixed inverting the tube. Lysed cell suspension was left for 5 minutes incubation at room temperature. After 5 minutes, 8 ml of Neutralization buffer NEU-EF was added to suspension and immediately mixed by inverting the tube. The resulting suspension was left for incubation on ice for 5 minutes. After 5 minutes, cell suspension was again mixed by inverting and poured onto previously equilibrated with 15 ml of Equilibration Buffer EQU-EF NucleoBond Xtra Column. When all suspension went through the filter, it was washed with 5 ml of Filter Wash Buffer Fil-EF and then removed. NucleoBond Xtra Column was washed 2 more times with Wash Buffer ENDO-EF, 35 ml of buffer was added once and 15 ml of buffer after. The column was emptied by gravity. Plasmid DNA was eluted with 5 ml of Elution Buffer ELU-EF and collected into a 50 ml tube. To precipitate the eluted plasmid DNA, 3,5 ml of room-temperature isopropanol was added to the tubes. Tubes were placed to -20°C for 1,5 h and later centrifuged at 5100 rpm for 30 minutes at 4°C. The supernatant was discarded after centrifugation and pellets were left to dry at room-temperature for 5-10 minutes. Later 3,5 ml of room-temperature 70% ethanol was added to the pellets and tubes were centrifuged at 5100 rpm for 5 minutes at room-temperature. The supernatant was carefully removed by pipetting and pellets were left to dry. When there was no more ethanol smell in the tube, pellets were redissolved in 100 µl of Endotoxin-Free Buffer TE-EF and plasmid DNA concentration was measured with a NanoDrop spectrometer. Colonies with the highest DNA concentration and optimal plasmid purity were sent for sequencing to ensure correctness of sequence. Tubes containing plasmid DNA (TGFBI and pcDNA) were stored at -20°C for enabling the conduction of further experiments.

3.1.3 Cell lines

HEK293 cell line (derived from human kidney embryo) originated from the American Type Culture Collection. **HaCaT** cell line (immortalized human keratinocytes) was a kind gift from Prof. Reet Kurg (Institute of Technology, University of Tartu). Human primary fibroblast culture was previously established in the laboratory by Dr. Klaas by explant culture method. Briefly, skin from healthy donors (collected from breast reduction surgeries, Tartu University Clinics; ethics permit 292/T-4) was cut into small pieces and adhered to Petri dishes. Skin pieces were covered in a growth medium that contained 89% DMEM with phenol red (Life Technologies Corporation, UK), 10% FBS (Life Technologies Corporation, Brazil) and 1% penicillin-streptomycin (Pen-Strep) solution (Life Technologies Corporation, USA). Cells were allowed to migrate from dermis for 10-14 days. Cells were passaged and stored as frozen stocks for further experiments. All cell cultures were grown at 37°C and 5% CO2 level in regular DMEM containing 89% DMEM, 10% Fetal Bovine Serum (FBS) and 1% Pen-Strep. Cell cultures were regularly passaged and transferred to new Petri dishes when they reached a high level of confluence.

3.1.4 Cell transfection

During the first day 2,2×10^6 HEK293 cells were plated into 4 separate 10cm-diameter Petri dishes containing 10 ml of growth medium. Cells were left for overnight growth.
On the next day cells were transfected by Turbofect transfection reagent (Thermo scientific, Lithuania). Two different transfection mixtures containing plasmid DNA were prepared, their composition is described in Table 1. Mixtures were mixed and incubated for 15 minutes at room-temperature.

Mixture	**Composition**
TGFBI (per 2 plates)	2 ml of DMEM medium (without phenol red dye), 20 µl of plasmid DNA solution(TGFBI), 33,2 µl of Turbofect reagent.
pcDNA (per 2 plates)	2 ml of DMEM medium (without phenol red dye), 20 µl of plasmid DNA solution (pcDNA), 33,2 µl of Turbofect reagent.

Table 1. Transfection mixture composition.

While the transfection mixture was incubating, the medium on plates was changed. There were 2 types of new medium with almost identical composition. The first medium contained 98% of serum free DMEM without phenol red dye (Life Technologies Corporation, USA), 1% of Insulin-Transferrin-Selenium (ITS, Life Technologies Corporation, USA) and 1% of Pen-Strep. The second medium included the same components with one exception, serum free DMEM contained phenol red dye. After 15 minutes passed, transfection mixtures were added onto the cells (1 ml per 1 plate). Eventually, there were 4 transfected cell plates, 2 of them (1 TGFBI and 1 pcDNA) containing medium with phenol red dye (required for further experiments) and other 2 plates containing no phenol red dye (required for later Western Blot analysis). HEK293 cells were left for 24 hour growth.

After 24 hours an additional amount of ITS (100 µl) was added onto the cells without changing the growth medium and cells were incubated at 37°C for 24 hours.

48 hours after transfection all cell medium was collected into 15 ml tubes. Medium containing phenol red dye was stored at 4°C for further experiments and medium without phenol red dye was mixed with 100 µl of 100x protease inhibitors (Thermo scientific, USA) and 40 µl of sodium azide with the final concentration of 0,04% and stored at 4°C for further usage.

3.1.5 Sample preparation for the protein expression analysis

3.1.5.1 Preparation of cell lysates (or cell lysis and protein extraction)

After the phenol red free media were collected, the cells were washed with 5 ml of phosphate buffered saline (PBS), lifted with 3 ml of trypsin (0,05%) solution and transferred to 50 ml tubes containing 15 ml of regular growth medium. Cell suspensions were centrifuged at 1200 rpm for 5 minutes at room-temperature. After the centrifugation supernatant was discarded, cell pellets were dissolved in 1 ml of PBS and transferred to new Eppendorf tubes. Tubes were centrifuged one more time at 5000 rpm for 10 minutes at 4°C. The supernatants were carefully discarded and 120 µl of lysis buffer (containing 1% of 100x protease inhibitors, 50 mM TRIS pH=8,0, 150 mM NaCl, 1% NP-40) was added to the pellets. Cells were incubated on ice for 1 hour and centrifuged for 15 minutes at 12000 rpm, at 4°C. The obtained supernatants were the final protein lysates, so they were transferred to new tubes and the protein concentration in lysates was measured using

the BCA protein assay kit (Thermo Scientific, USA) according to the manufacturer's instructions. 12 µl of protein lysate and 100 µl of Working Reaction (50 parts of reagent A:1 part of reagent B,) were mixed together, transferred to a 96-well plate and incubated for 30 minutes at 37°C. Later the protein concentration was measured using a spectrometer setted for 562 nm wavelength. Estimated protein concentrations were needed for further calculations of the correct loading of samples in Western Blot analysis.

3.1.5.2 Preparation of TGFBI-conditioned medium

The collected phenol red free media from transfected HEK293 cells were transferred into dialysis bags (Spectrum Medical Industries, TX); these bags were placed onto PEG40000 (polyethylene glycol M=40000g/mol) (SERVA, Germany) and removed from it when the volume of the contents of the bags did not exceed 250-300 µl. The bags were washed with MQ water and their contents were transferred to new Eppendorf tubes and precipitated with 5x volume of -20°C acetone. The precipitated proteins were centrifuged for 15 minutes at 15000 rpm, at 4°C. Final supernatant was discarded and the protein pellet was dissolved in 100 µl of MQ water and 30 µl of 4x Laemmli buffer (lysis buffer containing 40% glycerol, 0,25 M Tris-HCl pH=6,8, 8% SDS, 0,008% bromophenol blue and 20% β-mercaptoethanol). Samples were stored at -20°C for later Western Blotting.

3.1.6 Western Blot

3.1.6.1 Gel electrophoresis and transfer of proteins

First of all 10% resolving gel was prepared using 30% acrylamide mix (Thermo Fisher, Denmark), 1.5 M Tris-HCL base (pH 8,8), 10% Sodium dodecyl sulfate (SDS), 10% ammonium persulfate and TEMED. Resolving gel was solidified for approximately 45 minutes. Later a 5% stacking gel was added. The components of stacking gel are the same as in resolving gel with the exception in Tris base, it was replaced with 1.0 M Tris-HCL (pH 6,8).

For equal protein loading the correct volume of samples was calculated accordingly to before obtained protein concentration. The total volume of inserted samples was 37,5 µl consisting of cell lysates and 4x Laemmli buffer. Before loading the samples were heated at 99°C for 5 minutes and after centrifuged at 15000 rpm for 5 minutes. When the gel was ready, samples and 1kb PAGERuler (Thermo Scientific, Lithuania) were loaded to the gel.

The gel was running for 1,5-2 hours at 100V. After the proteins were separated by gel electrophoresis, they were transferred from the gel to polyvinylidene fluoride (PVDF) membrane (Thermo Scientific, USA) via wet electroblotting at 100 V approximately for 1 hour and 15 minutes.

3.1.6.2 Antibody binding

The PVDF membrane was firstly washed with 0,1% PBS-Tween20 (BioTop Naxo, Estonia) and then placed into 5 ml of blocking solution (0,1% PBS-Tween 2010, 3% bovine serum albumin (BSA) (AppliCam, Germany) and 3% nonfat skimmed milk powder) for 1 hour. After 1 hour, the previous blocking solution was poured away and replaced with a new blocking solution containing primary TGFBI Rabbit Polyclonal antibody (dilution 1:500) (ProteinTech, catalog number:10188-1-AP). The membrane was left on the shaker for overnight incubation at 4°C.

On the next day, the membrane was washed for 3×5 minutes with 0,1% PBS-Tween 20 and placed into a fresh blocking solution containing a secondary polyclonal goat anti-rabbit antibody (Dako, catalog number: P0448) (dilution 1:3000). The membrane was incubated in secondary antibody solution for 1 hour. After the incubation, it was again washed 3×5 minutes with 1x PBS-Tween 20 (0,1%) and placed into another blocking solution containing Streptavidin-AP (dilution 1:1000) (Dako, Denmark). After the last incubation, the membrane was washed 2×5 minutes with 1x PBS-Tween 20 (0,1%) and one more time in 1x Tris-Buffered Saline (TBS) for 10 minutes. Eventually, the membrane was placed into the NBT/BCIP(Thermo Scientific, USA) solution in order to visualise results. After the desired band appeared, reaction was stopped by rinsing the membrane with distilled water.

3.1.7 Wound healing assay

Before starting the wound healing assay, HaCaT cells and fibroblasts were plated on a 24-well plate. 10 wells of HaCaT cells were seeded (12000 cells into each well) and fibroblasts (15000 cells into each well) were distributed in the same manner. Cells were grown until they formed a confluent layer. 24 hours before starting the assay the regular DMEM medium was replaced with conditioned medium, containing 75% of DMEM and 25% of conditioned medium (containing pcDNA control or TGFBI protein). 5 wells from each cell line were supplied with conditioned medium containing pcDNA, the

supplementation with TGFBI conditioned medium was done with other 5 wells. On the next day, a scratch was done in each well using a sterile 200 ul pipette tip. Right after the scratch was done, 3 photos of each well were captured under the light microscope equipped with a 10x objective lens. Pictures were taken every 3 hours until the scratch was almost closed. The wound healing experiment with fibroblasts lasted for 12 hours and 24 hours for HaCaT cells. For HaCaT cells, pictures were taken every 3 hours until the 12 hour time point and 1 later time point after another 12 hours. The wound width on every picture for each timepoint was measured 3 times using the ImageJ programme, thereby obtaining the percentage value by which the wound is closed in each time interval. When the measurements were completed, the averages from replicates were taken and a Student's t-test was conducted to calculate the p-value, which resulting in a p-value would indicate if there was any significant difference in wound closure rate between cells that were and were not supplied with TGFBI. P-values more than 0,05 tend not to show significant difference. The experiment was performed twice.

3.1.7 Transwell migration assay

The transwell migration assay was conducted with fibroblasts. Fibroblasts were initially plated on a 10cm-diameter Petri dish containing regular growth medium. Once fibroblasts formed a confluent cell layer, they were passaged into 2 different wells of 6-well plate. 24 hours before starting the assay, the cells were stimulated with conditioned medium, the components of conditioned medium were the same as during wound healing assay. Conditioned medium for the first well included 25% of TGFBI and 25% of pcDNA for the second control well.

After 24 hours passed, fibroblasts were lifted by 0,05% trypsin and counted. Triplicates of 200 µl cell suspension containing 15000 fibroblasts in FBS-free DMEM containing 25% of conditioned medium (TGFBI or pcDNA) were prepared. 400 µl of regular DMEM (contains 10% of FBS) was added into 6 lower chambers of the 24-well transwell plate (6,5 mm diameter inserts, 8,0 µm pore size polycarbonate membrane, Corning Incorporated, USA). 200 µl of cell suspension was carefully pipetted into upper chambers. 3 wells contained TGFBI-conditioned medium, another 3 pcDNA-conditioned medium from transfected HEK293 cells.

24 hours later cells were fixed in methanol for 3 minutes, stained with 0,5% Coomassie

Brilliant Blue G-250 (Sigma-Aldrich) solution for 20 minutes and washed with MQ water several times to get rid of excessive dye. Fibroblasts that did not migrate through the membrane of the upper chamber were removed with a cotton bud. Pictures of each well were taken in 5 fields of view. Migrated fibroblasts were counted and a Student's t-test was conducted to calculate the p-value, which resulting value would show if there was any significant difference between the number of migrated cells that were or were not stimulated with TGFBI.

3.1.8 Tissue staining (indirect immunofluorescence)

Animal experiments were previously carried out by supervisors Mariliis Klaas and Kristina Mäemets-Allas who hold personal licences to perform animal experiments with rodents. 8-week-old C57/BL6 mice were used in experiments. 6-mm biopsy punch was used to create full-thickness dermal wounds in the dorsal skin of mice; the skin removed by this method was considered as day 0 (healthy control) in this study. To avoid contraction in the wound healing process a silicone ring (2-3 mm wide, with an inner diameter of 6mm) was applied around the wound. The mice were sacrificed at specified time points and the skin samples from healing wounds were embedded in O.C.T compound (Tissue-Tek, Sakura) and stored at -80°C. 10µm-thick frozen sections were cut for immunofluorescence.

Mouse skin sections with artificial wounds on different healing days (day 0/4/8) were used for tissue immunofluorescence analysis assay. Skin sections were taken out of -80°C and kept at room-temperature approximately for 10 minutes. Later sections were fixed with paraformaldehyde solution for 10 minutes and then washed 3×3 minutes in PBS. Following that skin sections were permeabilized in PBS containing 0,2% of Triton X-100 for 15 minutes at room-temperature. Then sections were again washed 3×3 minutes in PBS. Right after washing, mouse skin sections were incubated in a blocking buffer (PBS containing 5% of normal donkey serum, Sigma-Aldrich). Incubation was carried out in a humidified chamber. After 1 hour incubation, skin sections were incubated for 24 hours at 4°C in a blocking buffer with primary antibodies. Primary antibodies were TGFBI polyclonal antibody (produced in rabbit; dilution 1:100) (ProteinTech, catalog number: 10188-1-AP) and Ki-67 purified antibody (produced in rat; dilution 1:200, eBioscience, catalog number: 14-5698).

On the next day skin sections were washed 3×3 minutes in PBS and incubated for 1 hour at room-temperature in a blocking solution containing secondary antibodies. Secondary antibodies used were donkey anti-rabbit IgG H&L (Alexa Fluor 488; Life Technologies, catalog number: A21206) (dilution 1:1000) and donkey anti-rat IgG H&L (Alexa Fluor 594; Life Technologies, catalog number: A21209) (dilution 1:1000). After incubation with secondary antibodies, the skin sections were washed 3×3 minutes in PBS and then incubated for 2 minutes in PBS containing DAPI with a final concentration of 0,5 μg/ml (dilution 1:1000, Thermo Fisher). One more 3×3 minutes washing step in PBS was done. Then skin sections were mounted by applying drops of DAKO fluorescent solution (Dako North America, Inc., USA) onto them and covered with glass coverslip. Sections were placed at 4°C for overnight incubation. It is important to note that while incubating skin sections in fluorochrome-conjugated antibody solutions, they were kept away from light.
On the next day pictures were taken using a Olympus IX81 CellR microscope (Olympus Corporation, Hamburg, Germany) equipped with Hamamatsu Orca ER (Hamamatsu Photonics, Herrsching am Ammersee, Germany) camera and 10x or 40x objective and processed using Hokawo 2.1 software (Hamamatsu Photonics).

3.1.9 Proliferation assay (Luminescent cell viability assay)

In order to quantify the effect of TGFBI on cell proliferation, the number of viable cells was estimated every 24 hours for 5 timepoints (0h, 24h, 48h, 72h, 96h). Fibroblasts were plated into 96-well plate, 10 replicates for each measurement were needed (5 replicates stimulated with TGFBI conditioned medium, 5 replicates stimulated with pcDNA conditioned medium, 2 replicates with regular DMEM for negative control). The only exception in the number of replicates was during the first measurement, where there were only 5 replicates because measurements were done straight after plating cells. Each well contained 5000 fibroblasts. Every time point, 10 minutes before measuring the cell numbers, 100 μl of the ATP-binding luminescent reagent Cell Titer-Glo buffer (Promega, USA) was added into each well. After 10 minutes of incubation, cell suspensions were transferred to another specialized 96-well plate (Corning 96 Flat Bottom white, clear bottom) and cell luminescence of proliferating cells was measured by Infinite M200 Pro microplate reader. In order to determine whether TGFBI has an effect on fibroblast proliferation, Student's t-test was done.

4. RESULTS

4.1 Western Blot results

Western Blot was performed in order to verify that cell transfection with TGFBI-containing pcDNA plasmid had worked and TGFBI protein is expressed into HEK293 cell medium. Western Blot results can be seen on Figure 4. TGFBI protein is endogenously expressed in HEK293 cells due to it's transfection with TGFBI plasmid vector and appears as a band of approximately 68 kDa size. Cell lysate, which was transfected with pcDNA vector does not appear the same line, but shows some other ones, this might be due to unspecific binding and natural synthesis of other different proteins in HEK293 cells. TGFBI protein is strongly expressed into TGFBI conditioned medium. The band for TGFBI conditioned medium "sagged down" due to the high presence of TGFBI protein although the conditioned medium was precipitated with ethanol. In this regard, the current location of the band was considered to be at its edges with the size around 68 kDa. No substantial bands appeared in pcDNA-conditioned medium.

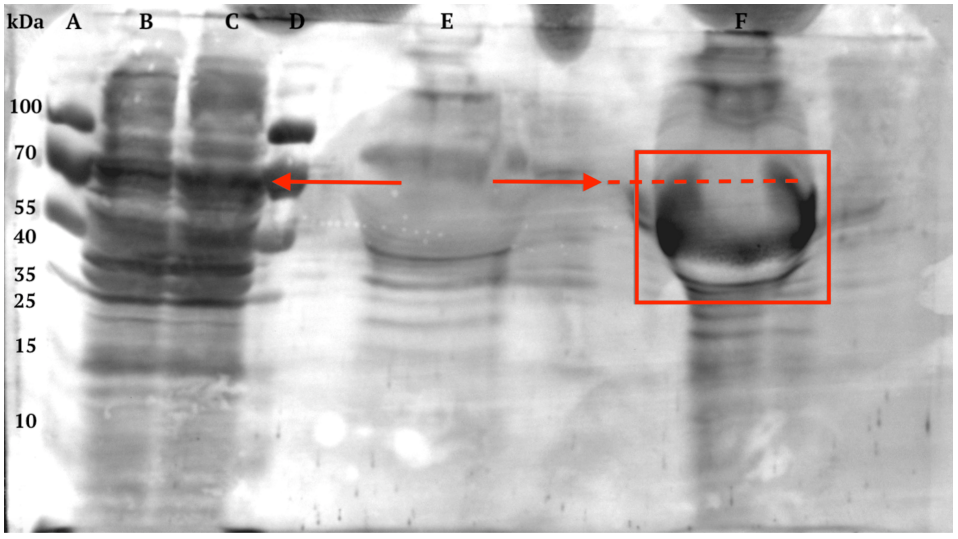

Figure 4. Western Blot result proving that TGFBI protein is expressed into TGFBI conditioned medium and in HEK293 cells that were transfected with TGFBI plasmid vector (A - marker; B - HEK293 cells lysate containing pcDNA; C - HEK293 cells lysate containing TGFBI; D - marker; E - HEK293 cell medium containing pcDNA; F - HEK293 cell medium containing TGFBI).

4.2 The effect of TGFBI on cell migration

In order to examine the effect of TGFBI protein on cell migration, two different assays were performed.

The scratch-wound healing experiment results show that TGFBI protein does not promote migration of HaCaT cells and fibroblasts (Figure 5 - 6A, 6B). This experiment was repeated twice. The graphs showing results of the first repetition of the experiment are demonstrated on Figure 5. Fibroblasts that were stimulated with TGFBI migrate faster, reaching an average 62,6% of wound closure at 12 hours time point, while wound closure percentage at the same time point for pcDNA treated fibroblasts averaged 48,8% (Figure 5A). From the first sight it seems a tendency that TGFBI promotes cell migration but the variation in measurements was very high, varying at some places for more than 35%. Therefore it was decided not to regard these data as statistically significant as the p-values emerged to be higher than 0,05. Such fluctuations in wound closure percentage might be caused by initially unevenly executed scratches, which led to errors in the measurement process. In the same way as fibroblasts, during the first try, HaCaT cells that were stimulated with TGFBI were migrating faster than those stimulated with pcDNA conditioned medium, reaching an average 25,3% of wound closure at the 12 hours time point. At two time points (9 and 12 hours) TGFBI appeared to promote HaCaT cells migration; this was proved by conducting the Student's t-test (p-value<0,05). Wound closure percentage of HaCaT cells treated with pcDNA conditioned medium reached a value of 22% (Figure 5B). P-values calculated from 3, 6 and 24 hour time points appeared to be higher than 0,05 meaning that the difference is not statistically significant. Overall, it is possible to suggest that TGFBI has some effect on migration of **HaCaT cells**.

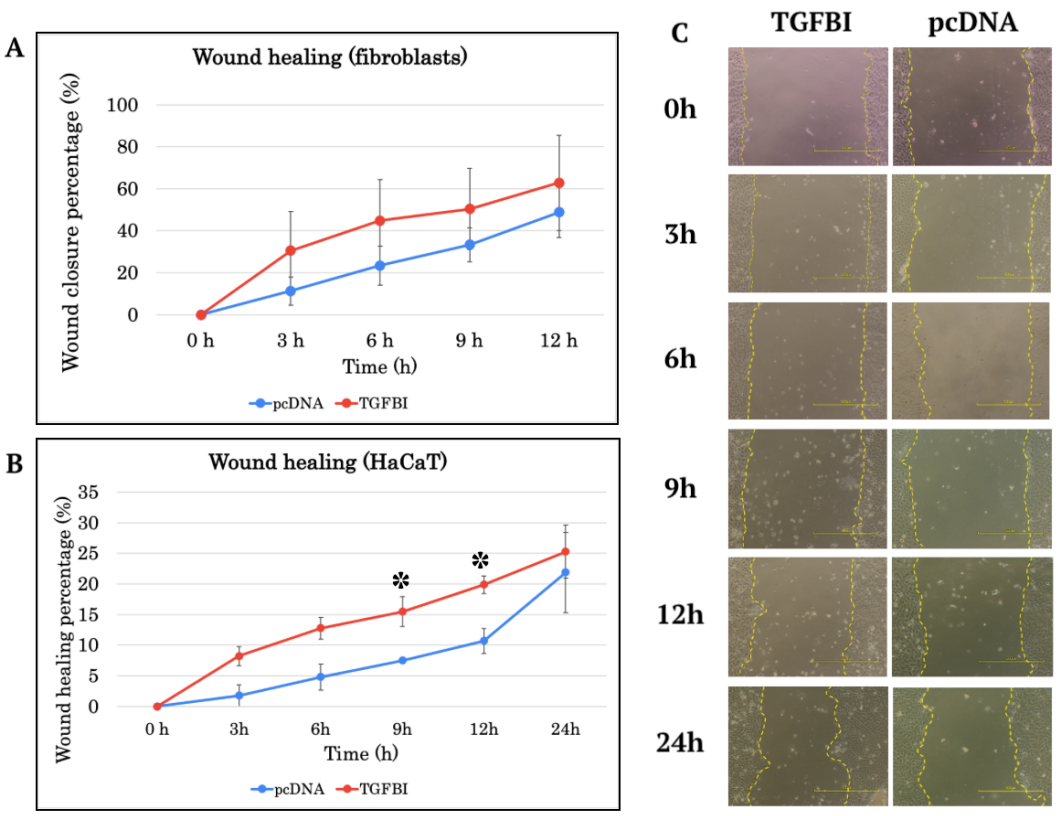

Figure 5. Wound healing assay results №1 (A - fibroblasts; B - HaCaT cells; C - example of the process of wound closure from the first experiment with HaCaT cells). TGFBI promoted migration of HaCaT cells at two time points (9 and 12 hour) but seemed to have no effect on fibroblast migration. Error bars represent the calculated standard deviation in order to show some uncertainties in conducted measurement.

The graphs showing the results from the second repetition of the experiment (Figure 6) demonstrate that fibroblasts that were stimulated with TGFBI migrate slightly faster, reaching 36% of wound closure at 12 hours time point, while wound closure percentage at the same time point for pcDNA treated fibroblasts appeared to be 26,5%. After conducting the Student's t-test, p-value for each time point emerged to be higher than 0,05, which means that difference in wound closure percentage between fibroblasts stimulated with pcDNA and TGFBI conditioned medium was not statistically important (Figure 6A). Migration of HaCaT cells was almost identical during the 12 hour period (pcDNA and TGFBI). At the 24 hour time point HaCaT cells stimulated with TGFBI conditioned medium reached 31,8% of wound closure and 30% for cells treated with pcDNA conditioned medium. P-value appeared to be much higher than 0,05, which means that TGFBI has no statistically significant effect on HaCaT cell migration as well (Figure 6B).

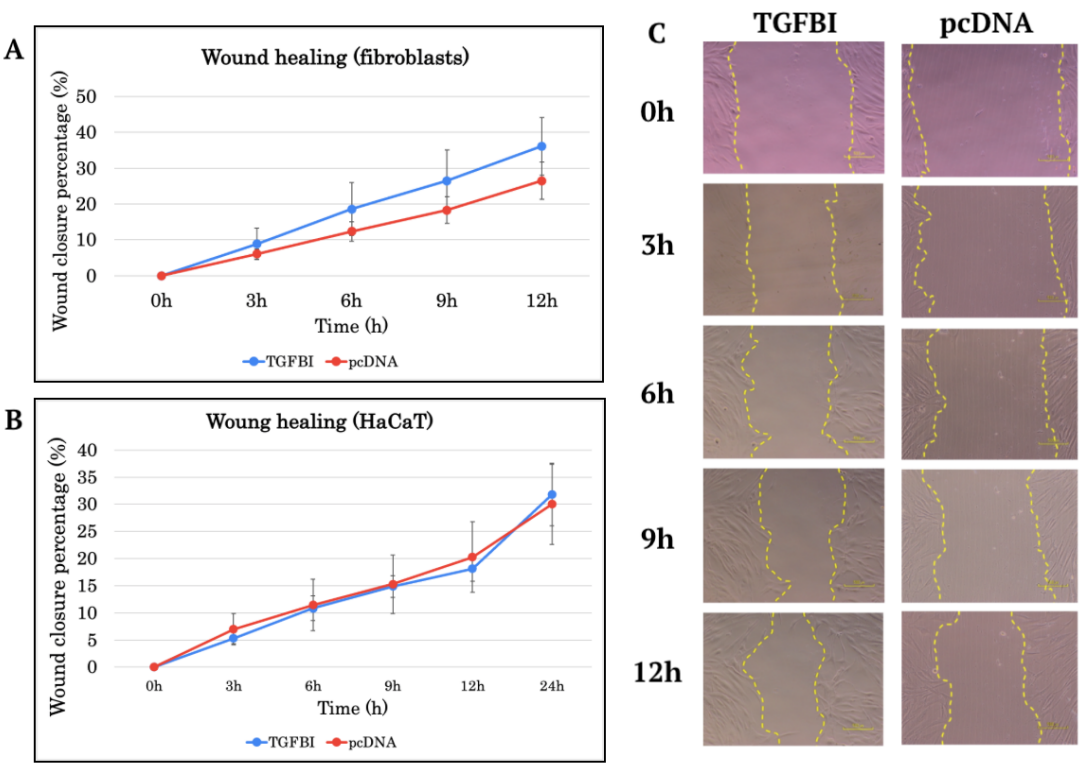

Figure 6. Wound healing assay results №2 (A - fibroblasts; B - HaCaT cells; C - process of wound closure from second experiment with fibroblasts). Error bars represent the calculated standard deviation in order to show some uncertainties in conducted measurement. TGFBI seemed to have no statistically important effect on cell migration.

In order to be more confident that TGFBI influences cell migration, a **transwell migration experiment** was carried out. The experiment was carried out twice, but one of the attempts was unsuccessful. Fibroblasts did not migrate through the membrane at all, most likely due to an error during the experiment. An error in the calculations or an incomplete fixation of cells with methanol could be the reason for the failure.

Based on the results of repeating the experiment (Figure 7), TGFBI slightly promoted the migration of fibroblasts through the membrane, however, after conduction of Student's t-test, it turned out that the p-value was greater than 0,05 and therefore this result could not be considered statistically significant.

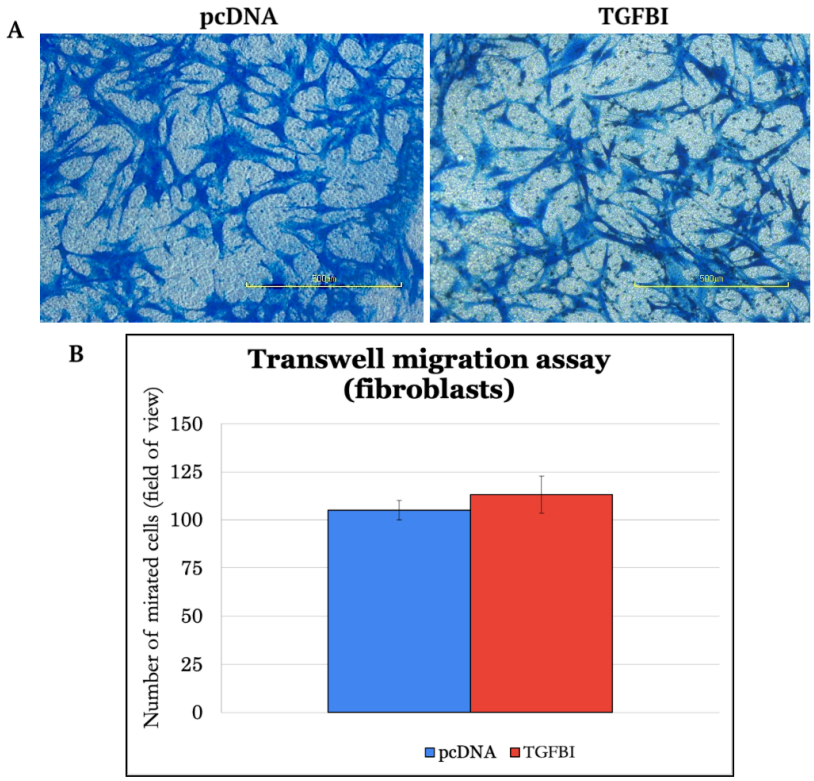

Figure 7. Picture A - A representative image of migrated fibroblasts under a light microscope with 10x objective lens; graph B - results of transwell migration assay. Bars represent the average number of cells viable in one field of view. Error bars represent the calculated standard deviation in order to show some uncertainties in conducted measurement.

Taking into account all that were obtained from these two types of experiments, it should be considered that TGFBI protein has no statistically significant effect on migration of fibroblasts. TGFBI protein showed some promoting effect on HaCaT cells during the first repetition of wound healing experiment and did not appear any effect during the second repetition meaning that it sometimes may stimulate HaCaT cells migration, but obtained results are not enough to state this fact. More repetitions must be done in order to consider the promoting effect of TGFBI on HaCaT cells statistically significant.

4.3 TGFBI effect on fibroblast proliferation

In order to test the effect of TGFBI protein on fibroblast proliferation, cell viability measurements were performed on multiple timepoints. Cell Titer-Glo assay that determines the number of proliferating cells by detecting ATP in viable cells was used for

this purpose. This luminescence-conjugated assay allows to estimate the number of metabolically active cells by measuring the level of luminescence from the cell sample. The results of this experiment can be seen on Figure 8. Fibroblasts stimulated with a TGFBI conditioned medium proliferated almost on the same level as fibroblasts stimulated with pcDNA conditioned medium. Only on the second day of incubation, the proliferation of fibroblasts stimulated with a TGFBI conditioned medium increased enough to result in a p-value of less than 0.05. However, the p-value calculated for all other time points turned out to be less than 0.05, respectively, the result of this experiment is considered to be statistically insignificant.

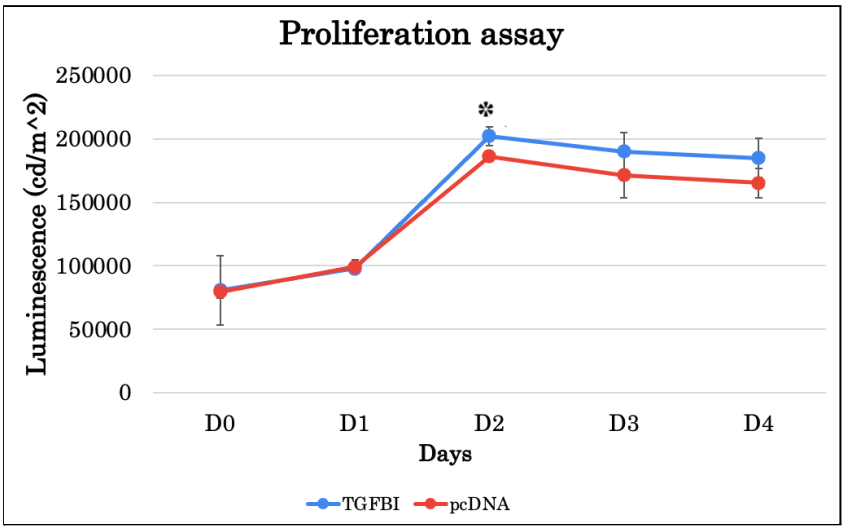

Figure 8. Results of the proliferation assay. Lines on the graph show the number of proliferating cells at each time point (0, 24, 48, 72, 96 hours). On the second day of the experiment fibroblasts stimulated with TGFBI showed higher levels of proliferation than those, which were stimulated with pcDNA. Error bars visualize the standard deviation calculated for each time interval.

4.5 TGFBI expression in mouse skin

In order to characterize the TGFBI protein expression in skin, an immunofluorescence analysis of healing full-thickness skin wounds was performed. For the experiment, several sections of mouse skin were selected at different stages of the wound healing process (day 0 - healthy skin, day 4 of healing and day 8 of healing).

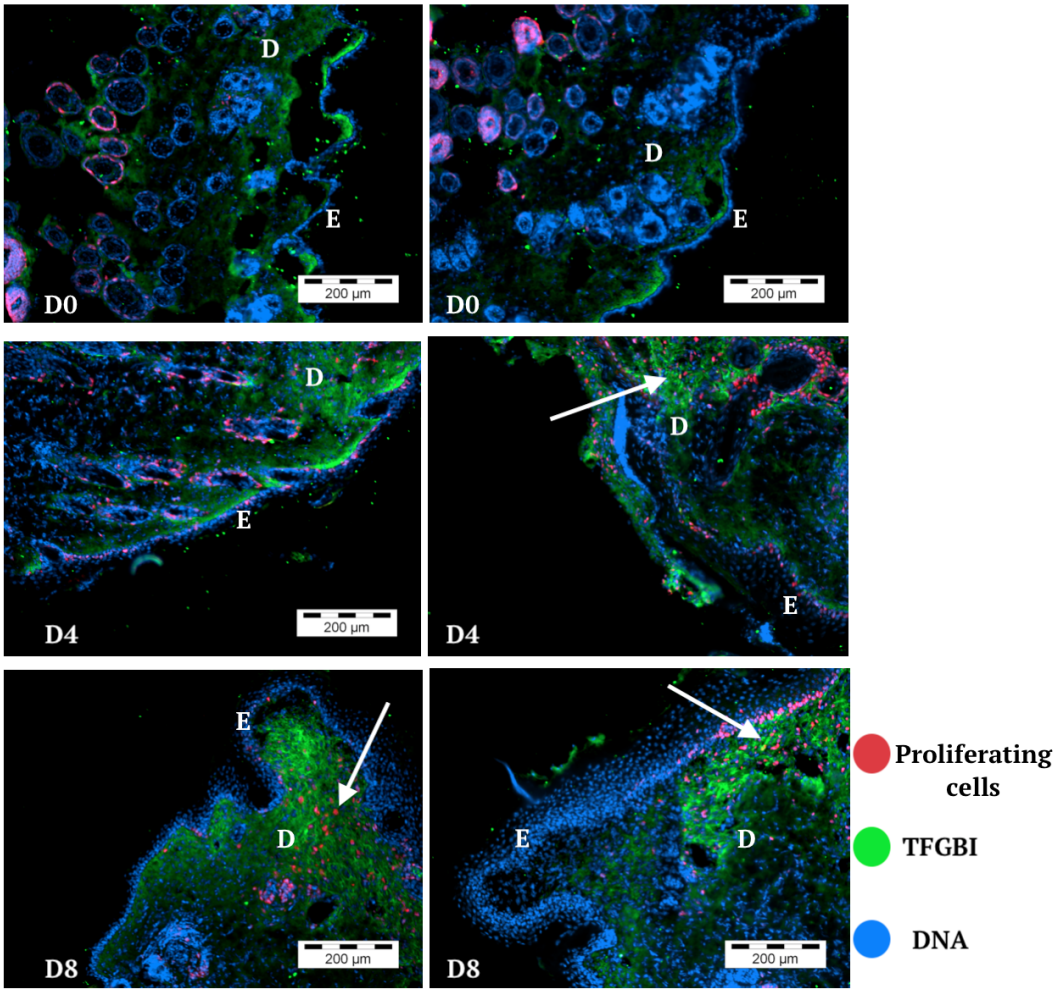

Figure 9. Results of immunofluorescence analysis. **D0** - healthy skin; epiremis (E) and dermis (D). **D4** - 4th day of wound healing process; epiremis (E) and dermis (D). Coexpression of TGFBI and proliferating cells marked with an arrow on the second picture. **D8** - 8th day of wound healing process; epiremis (E) and dermis (D). Coexpression of TGFBI and proliferating cells marked with arrows.

TGFBI polyclonal antibody was used for detecting the expression of TGFBI protein. It is shown on Figure 9 that TGFBI is expressed in the ECM of the dermis during the wound healing process, as well as in the healthy skin. It is possible to notice that TGFBI expression is stronger in the area under the epidermis during the wound healing process meaning that TGFBI might be upregulated in wound healing (Figure 9-D4, 9-D8). Ki-67 marker was used to detect proliferating cells (red). Figures 9-D0 demonstrate that proliferating cells are concentrated around the hair follicles due to the fact that hair follicles are constantly amenable to the regeneration process. On the images from day 4 of healing (Figure 9-D4), proliferating cells can be found in the epidermis area. Most likely

these cells are keratinocytes, which are actively involved in the creation of a new epithelial layer of the skin. Co-localization of proliferating cells and expressed TGFBI can be observed during 4th and 8th healing days (Figure 9-D4, 9-D8). On the 8th day of healing (Figure 9-D8), a certain number of proliferating cells can be observed in the dermis, while in the epidermal layer there are fewer of them. This may be due to the process of re-establishment of the dermal extracellular matrix. Judging by the simultaneous presence of proliferating cells in the dermis and epidermis, it can be assumed that the process of re-epithelialization and restoration of the extracellular matrix are parallel to each other.

DISCUSSION

The effect of TGFBI protein on skin regeneration and wound healing by accelerating cell proliferation and migration was studied in this research project.

Two types of experiments have been performed to study the effect of TGFBI protein on cell migration. One of them was the wound healing assay. The experiment was carried out twice and from its results it was concluded that TGFBI has no statistically significant effect on cell migration (Figures 5-6). The results of wound healing assay with HaCaT cells are partially comparable with the results of studies carried out by Bae *et al*. (2002) due to the fact that overall HaCaT cells stimulated with TGFBI conditioned medium were migrating slightly faster than those stimulated with pcDNA reaching statistically significant difference at 2 time points, nevertheless it was ultimately accepted that these data were insufficient for an accurate statement that TGFBI accelerates HaCaT cell migration. Bae *et al*. (2002) showed in their study that TGFBI promotes migration of keratinocytes through the interaction of NKDIL and EPDIM motifs with integrin α3β1. A possible reason for this discrepancy in the results is that Bae *et al*. (2002) were using normal human keratinocytes to test the effect of TGFBI on cell migration instead of HaCaT cells. Despite the fact that HaCaT cells are very similar in their properties to normal human keratinocytes, they can still have some different characteristics.

The fact that TGFBI protein has no effect on fibroblast migration was also confirmed by conducting a migration assay. Despite the fact that cells stimulated with TGFBI protein migrated across the transwell membrane in a larger number than cells stimulated with pcDNA, the difference between their number was considered statistically insignificant (Figure 7).

In order to study the effect of TGFBI on fibroblast proliferation, a proliferation assay was performed. During this experiment, the number of viable cells stimulated with TGFBI conditioned medium was almost the same for the first 24 hours and during the remaining time exceeded the number of cells stimulated by the pcDNA conditioned medium. However, after a statistical test, this difference was considered to be insignificant. Only at the 48 hour point, the proliferation of fibroblasts stimulated with TGFBI conditioned medium was statistically higher than that of cells stimulated with pcDNA (Figure 8); nevertheless, this fact is not enough to confirm the fact that TGFBI promotes fibroblast proliferation. Xiao (2012) also investigated the effect of TGFBI conditioned medium on fibroblast proliferation. In this study, through several different experiments (including

proliferation assay), it was shown that TGFBI influences the proliferation of fibroblasts by promoting it. The results of the study by Xiao (2012) can be considered partially comparable with the results of this study, since the proliferation of fibroblasts stimulated with TGFBI was still higher than the proliferation of those stimulated with pcDNA, although it had no statistical significance. One of the reasons why the results of this study do not agree with the data of Xiao (2012) may be the use of different cell lines. Although fibroblasts were used in both studies, cells were obtained from different organisms; Xiao, 2012 used NIH3T3 cell line derived from mouse embryonic fibroblasts, while human derived fibroblasts were used during current research. In addition to that, the reason for this result could simply be the quality of the TGFBI conditioned medium, since this experiment was carried out in the last turn and a considerable amount of time has passed since the moment of transfection, some of the proteins could denature and their effect on cells could become weaker.

Besides the experiments described above, immunofluorescence analysis was performed to determine the site of TGFBI expression in the skin. For this experiment, mouse skin was used at several stages of healing. It has been shown that TGFBI is expressed in the extracellular matrix of the dermis, it is equally distributed in healthy skin and more concentrated in the upper dermis during the healing process meaning that TGFBI expression might be upregulated during the wound healing process (Figure 9). The expression of TGFBI in skin was studied by Bae *et al*. (2002) they investigated that TGFBI protein is expressed in the upper layer of dermis. Research done by LeBaron *et al*. (1995) showed that TGFBI is expressed in normal skin, especially in the papillary dermis.

Co-expression of TGFBI and proliferating cells can be observed in the site of the future epidermis (Figure 9D4, 9D8); the role of TGFBI at this moment may be to support proliferating cells by influencing their mitotic division and their migration (Strodtbeck, 2001).

To sum up all mentioned above, it is possible to conclude that TGFBI is indeed expressed in the ECM, but seems to have no statistically significant effect on the migration and proliferation of HaCaT cells and fibroblasts. The results of this study are partially comparable to the results of previous studies, but still contradicts with them in final results. More repetitions of all experiments have to be done in order to specify the effect of TGFBI protein on cell migration and proliferation.

SUMMARY

The main aim of this study was to test the effect of TGFBI on skin regeneration and wound healing. At the beginning of the work, it was hypothesized that TGFBI affects the regeneration of the skin and wound healing by accelerating the migration and proliferation of keratinocytes and fibroblasts. In order to test this hypothesis, several goals were defined.

The first goal was to study the site of TGFBI expression in the skin by immunofluorescence analysis. It was found that TGFBI is expressed in the extracellular matrix of the dermis of both healthy and healing skin.

The next goal was to test the effect of TGFBI on cell migration. For this, the following experiments were carried out: scratch-wound healing assay and the transwell migration assay. In general, the results of the wound healing experiment showed that TGFBI had no statistically significant effect on cell migration. The results of the transwell migration experiment were identical to those of the wound healing experiment.

The final goal was to test the effect of TGFBI on cell proliferation. An experiment was carried out to find out what effect TGFBI has on cell proliferation. The results showed that TGFBI had no statistically significant effect on cell proliferation.

The results of conducted experiments are inconsistent with the results of previous studies. To obtain more meaningful results, more experiments should be carried out.

The hypothesis put forward at the beginning of the study was refuted.

REFERENCES

Bae, J. S., Lee, S. H., Kim, J. E., Choi, J. Y., Park, R. W., Yong Park, J., Park, H. S., Sohn, Y. S., Lee, D. S., Bae Lee, E., & Kim, I. S. (2002). βig-h3 supports keratinocyte adhesion, migration, and proliferation through α3β1 integrin. *Biochemical and Biophysical Research Communications*, *294*(5), 940–948. https://doi.org/10.1016/s0006-291x(02)00576-4

Barbieri, J., Wanat, K., & Seykora, J. (2014). Skin: Basic Structure and Function. *Pathobiology of Human Disease*, 1134–1144. https://doi.org/10.1016/b978-0-12-386456-7.03501-2

Bosman, F. T., & Stamenkovic, I. (2003). Functional structure and composition of the extracellular matrix. *The Journal of Pathology*, *200*(4), 423–428. https://doi.org/10.1002/path.1437

Broughton, G., Janis, J. E., & Attinger, C. E. (2006a). The Basic Science of Wound Healing. *Plastic and Reconstructive Surgery*, *117*(SUPPLEMENT), 12S-34S. https://doi.org/10.1097/01.prs.0000225430.42531.c2

Broughton, G., Janis, J. E., & Attinger, C. E. (2006b). Wound Healing: An Overview. *Plastic and Reconstructive Surgery*, *117*(SUPPLEMENT), 1e-S. https://doi.org/10.1097/01.prs.0000222562.60260.f9

Chen, C. L., Huang, W. Y., Wang, E. H. C., Tai, K. Y., & Lin, S. J. (2020). Functional complexity of hair follicle stem cell niche and therapeutic targeting of niche dysfunction for hair regeneration. *Journal of Biomedical Science*, *27*(1). https://doi.org/10.1186/s12929-020-0624-8

Chu, D. H. (2008). Development and Structure of Skin [E-book]. In K. Wolff, D. Leffell, A. Paller, B. Gilchrest, S. Katz, & L. Goldsmith (Eds.), *Dermatology in general medicine* (8th ed., pp. 57–73). McGraw-Hill Education / Medical. https://accessmedicine.mhmedical.com/content.aspx?sectionid=41138700&bookid=392#56021466

Eckert, R. L., Efimova, T., Dashti, S. R., Balasubramanian, S., Deucher, A., Crish, J. F., Sturniolo, M., & Bone, F. (2002). Keratinocyte Survival, Differentiation, and Death: Many Roads Lead to Mitogen-Activated Protein Kinase. *Journal of Investigative Dermatology Symposium Proceedings*, *7*(1), 36–40. https://doi.org/10.1046/j.1523-1747.2002.19634.x

Frantz, C., Stewart, K. M., & Weaver, V. M. (2010). The extracellular matrix at a glance. *Journal of Cell Science*, *123*(24), 4195–4200. https://doi.org/10.1242/jcs.023820

Gonzalez, A. C. D. O., Costa, T. F., Andrade, Z. D. A., & Medrado, A. R. A. P. (2016). Wound healing - A literature review. *Anais Brasileiros de Dermatologia*, *91*(5), 614–620. https://doi.org/10.1590/abd1806-4841.20164741

Haake, A., Scott, G. A., & Holbrook, K. A. (2001). Structure and Function of the Skin: Overview of Epidermis and Dermis [E-book]. In R. K. Freinkel & D. T. Woodley (Eds.), *The Biology of the Skin* (1st ed., pp. 19–45). CRC Press. https://books.google.ee/books?id=HxYN3db9R3MC&printsec=copyright&hl=ru#v=onepage&q&f=false

Houben, E., De Paepe, K., & Rogiers, V. (2006). A Keratinocyte's Course of Life. *Skin Pharmacology and Physiology*, *20*(3), 122–132. https://doi.org/10.1159/000098163

Hynes, R. O. (2009). The Extracellular Matrix: Not Just Pretty Fibrils. *Science*, *326*(5957), 1216–1219. https://doi.org/10.1126/science.1176009

Ji, S., Zhu, Z., Sun, X., & Fu, X. (2021). Functional hair follicle regeneration: an updated review. *Signal Transduction and Targeted Therapy*, *6*(1). https://doi.org/10.1038/s41392-020-00441-y

Kanitakis J. (2002). Anatomy, histology and immunohistochemistry of normal human skin. *European journal of dermatology : EJD*, *12*(4), 390–401

Kirsner, R. S., & Eaglstein, W. H. (1993). The Wound Healing Process. *Dermatologic Clinics*, *11*(4), 629–640. https://doi.org/10.1016/s0733-8635(18)30216-x

Labat-Robert, J., Bihari-Varga, M., & Robert, L. (1990). Extracellular matrix. *FEBS Letters*, *268*(2), 386–393. https://doi.org/10.1016/0014-5793(90)81291-u

LeBaron, R. G., Bezverkov, K. I., Zimber, M. P., Pavelec, R., Skonier, J., & Purchio, A. F. (1995). βIG-H3, a Novel Secretory Protein Inducible by Transforming Growth Factor-β, Is Present in Normal Skin and Promotes the Adhesion and Spreading of Dermal Fibroblasts In Vitro. *Journal of Investigative Dermatology*, *104*(5), 844–849. https://doi.org/10.1111/1523-1747.ep12607024

Losquadro, W. D. (2017). Anatomy of the Skin and the Pathogenesis of Nonmelanoma Skin Cancer. *Facial Plastic Surgery Clinics of North America*, *25*(3), 283–289. https://doi.org/10.1016/j.fsc.2017.03.001

Melott, A. J., Zamierowski, D. S., & Andrews, B. T. (2016). Phases of wound healing process [Illustration]. In *Negative Pressure Wound Therapy in Maxillofacial Applications*.

Moll, I., Kuhn, C., & Moll, R. (1995). Cytokeratin 20 Is a General Marker of Cutaneous Merkel Cells While Certain Neuronal Proteins Are Absent. *Journal of Investigative Dermatology*, *104*(6), 910–915. https://doi.org/10.1111/1523-1747.ep12606183

Moll, R., Franke, W. W., Schiller, D. L., Geiger, B., & Krepler, R. (1982). The catalog of human cytokeratins: Patterns of expression in normal epithelia, tumors and cultured cells. *Cell*, *31*(1), 11–24. https://doi.org/10.1016/0092-8674(82)90400-7

Monteiro-Riviere, N. (2005). Structure and Function of Skin. *Dermal Absorption Models in Toxicology and Pharmacology*, 1–19. https://doi.org/10.1201/9780203020821.ch1

Nummela, P., Lammi, J., Soikkeli, J., Saksela, O., Laakkonen, P., & Hölttä, E. (2012). Transforming Growth Factor Beta-Induced (TGFBI) Is an Anti-Adhesive Protein Regulating the Invasive Growth of Melanoma Cells. *The American Journal of Pathology*, *180*(4), 1663–1674. https://doi.org/10.1016/j.ajpath.2011.12.035

O'Brien, E. R., Bennett, K. L., Garvin, M. R., Zderic, T. W., Hinohara, T., Simpson, J. B., Kimura, T., Nobuyoshi, M., Mizgala, H., Purchio, A., & Schwartz, S. M. (1996). Beta βig-h3, a Transforming Growth Factor–β–Inducible Gene, Is Overexpressed in Atherosclerotic and Restenotic Human Vascular Lesions. *Arteriosclerosis, Thrombosis, and Vascular Biology*, *16*(4), 576–584. https://doi.org/10.1161/01.atv.16.4.576

Reinboth, B., Thomas, J., Hanssen, E., & Gibson, M. A. (2006). Beta βig-h3 Interacts Directly with Biglycan and Decorin, Promotes Collagen VI Aggregation, and Participates in Ternary Complexing with These Macromolecules. *Journal of Biological Chemistry*, *281*(12), 7816–7824. https://doi.org/10.1074/jbc.m511316200

Runager, K., Enghild, J. J., & Klintworth, G. K. (2008). Focus on molecules: Transforming growth factor beta induced protein (TGFBIp). *Experimental Eye Research*, *87*(4), 298–299. https://doi.org/10.1016/j.exer.2007.12.001

Schultz, G. S., Chin, G. A., Moldawer, L., & Diegelmann, R. F. (2011). *Principles of Wound Healing*. Mechanisms of Vascular Disease: A Reference Book for Vascular Specialists. https://www.ncbi.nlm.nih.gov/books/NBK534261/

Schuppan, D., & Riecken, E. (1990). Molecules of the Extracellular Matrix: Potential Role of Collagens and Glycoproteins in Intestinal Adaptation. *Digestion*, *46*(2), 2–11. https://doi.org/10.1159/000200360

Smith, L. T., & Holbrook, K. A. (1986). Embryogenesis of the Dermis in Human Skin. *Pediatric Dermatology*, *3*(4), 271–280. https://doi.org/10.1111/j.1525-1470.1986.tb00525.x

Strodtbeck, F. (2001). Physiology of wound healing. *Newborn and Infant Nursing Reviews*, *1*(1), 43–52. https://doi.org/10.1053/nbin.2001.23176

Thapa, N., Lee, B. H., & Kim, I. S. (2007). TGFBIp/βig-h3 protein: A versatile matrix molecule induced by TGF-β. *The International Journal of Biochemistry & Cell Biology*, *39*(12), 2183–2194. https://doi.org/10.1016/j.biocel.2007.06.004

Theocharis, A. D., Skandalis, S. S., Gialeli, C., & Karamanos, N. K. (2016). Extracellular matrix structure. *Advanced Drug Delivery Reviews*, *97*, 4–27. https://doi.org/10.1016/j.addr.2015.11.001

Velnar, T., Bailey, T., & Smrkolj, V. (2009). The Wound Healing Process: An Overview of the Cellular and Molecular Mechanisms. *Journal of International Medical Research*, *37*(5), 1528–1542. https://doi.org/10.1177/147323000903700531

Watt, F. M. (1998). Epidermal stem cells: markers, patterning and the control of stem cell fate. *Philosophical Transactions of the Royal Society of London. Series B: Biological Sciences*, *353*(1370), 831–837. https://doi.org/10.1098/rstb.1998.0247

Ween, M. P., Oehler, M. K., & Ricciardelli, C. (2012). Transforming Growth Factor-Beta-Induced Protein (TGFBI)/(βig-H3): A Matrix Protein with Dual Functions in Ovarian Cancer. *International Journal of Molecular Sciences*, *13*(8), 10461–10477. https://doi.org/10.3390/ijms130810461

Wise, S. G., & Weiss, A. S. (2009). Tropoelastin. *The International Journal of Biochemistry & Cell Biology*, *41*(3), 494–497. https://doi.org/10.1016/j.biocel.2008.03.017

Wong, R., Geyer, S., Weninger, W., Guimberteau, J. C., & Wong, J. K. (2015). The dynamic anatomy and patterning of skin. *Experimental Dermatology*, *25*(2), 92–98. https://doi.org/10.1111/exd.12832

Xiao, L. (2012). TGF-beta 1 induced fibroblast proliferation is mediated by the FGF-2/ERK pathway. *Frontiers in Bioscience*, *17*(7), 2667. https://doi.org/10.2741/4077

Yanagishita, M. (1993). Function of proteoglycans in the extracellular matrix. *Pathology International*, *43*(6), 283–293. https://doi.org/10.1111/j.1440-1827.1993.tb02569.x

Young, A., & McNaught, C. E. (2011). The physiology of wound healing. *Surgery (Oxford)*, *29*(10), 475–479. https://doi.org/10.1016/j.mpsur.2011.06.011

Yue, B. (2014). Biology of the Extracellular Matrix. *Journal of Glaucoma*, *23*, S20–S23. https://doi.org/10.1097/ijg.0000000000000108

Zeng, Q., Macri, L., Prasad, A., Clark, R., Zeugolis, D., Hanley, C., Garcia, Y., Pandit, A., Leavesley, D., Stupar, D., Fernandez, M., Fan, C., & Upton, Z. (2017). Skin Tissue

Engineering. *Comprehensive Biomaterials II*, 334–382. https://doi.org/10.1016/b978-0-12-803581-8.10157-2

Zhao, Y. L., Piao, C. Q., & Hei, T. K. (2002). Downregulation of Betaig-h3 gene is causally linked to tumorigenic phenotype in asbestos treated immortalized human bronchial epithelial cells. *Oncogene*, *21*(49), 7471–7477. https://doi.org/10.1038/sj.onc.1205891

INTERNET SOURCES

Brown, T. M., & Krishnamurthy, K. (2020). *Histology, Dermis*. StatPearls. https://www.ncbi.nlm.nih.gov/books/NBK535346/

Healthwise Staff. (2020). *Cross section of skin, skin layers* [Illustration]. Alberta. https://myhealth.alberta.ca/Health/pages/conditions.aspx?hwid=tp10137

Melott, A. J., Zamierowski, D. S., & Andrews, B. T. (2016). Phases of wound healing process [Illustration]. In *Negative Pressure Wound Therapy in Maxillofacial Applications*.

Lawton, S. (2019). *Skin 1: the structure and functions of the skin*. Nursing Times. https://www.nursingtimes.net/clinical-archive/dermatology/skin-1-the-structure-and-functions-of-the-skin-25-11-2019/

Lopez-Ojeda, W., Pandey , A., Alhajj, M., & Oakley, A. M. (2020). *Anatomy, Skin (Integument)*. In *StatPearls*. StatPearls Publishing. https://pubmed.ncbi.nlm.nih.gov/28723009/

Smith, Y. B. (2019, February 27). *What is the Dermis?* News-Medical.Net. https://www.news-medical.net/health/What-is-the-Dermis.aspx

Yousef, H., Alhajj, M., & Sharma, S. (2017). *Anatomy, Skin (Integument), Epidermis*. Europe PMC. https://europepmc.org/article/nbk/nbk470464#free-full-text

NON-EXCLUSIVE LICENCE TO REPRODUCE THESIS AND MAKE THESIS PUBLIC

I,

Oleksandra Dranova

1. herewith grant the University of Tartu a free permit (non-exclusive licence) to

reproduce, for the purpose of preservation, including for adding to the DSpace digital archives until the expiry of the term of copyright,

The role of TGFBI in wound healing and skin regeneration,

supervised by Mariliis Klaas and Kristina Mäemets-Allas.

2. I grant the University of Tartu a permit to make the work specified in p. 1 available to the public via the web environment of the University of Tartu, including via the DSpace digital archives, under the Creative Commons licence CC BY NC ND 3.0, which allows, by giving appropriate credit to the author, to reproduce, distribute the work and communicate it to the public, and prohibits the creation of derivative works and any commercial use of the work until the expiry of the term of copyright.

3. I am aware of the fact that the author retains the rights specified in p. 1 and 2.

4. I certify that granting the non-exclusive licence does not infringe other persons' intellectual property rights or rights arising from the personal data protection legislation.

Oleksandra Dranova

20/05/2021